

Fabrication of semi-conductive ceramics by combination of gelcasting and reduction sintering

MINORU TAKAHASHI*, KOICHIRO ADACHI, RUBEN L. MENCHAVEZ,
MASAYOSHI FUJI

Nagoya Institute of Technology, Asahigaoka, 10-6-29 Tajimi, Gifu, Japan 507-0071
E-mail: m-takahashi@nitech.ac.jp

In this study, we propose a new process to fabricate electrically semi-conductive alumina by the combination of gelcasting and reduction sintering. The process is similar to the conventional gelcasting method except for varying amounts of methacrylamide monomer dosages at 2.83, 5.50, and 8.04 wt% relative to the mass of the slurry. Correspondingly, the rheological evaluation of aqueous slurry was conducted. The resulting fluidity exhibited that monomer dosage until 8.04 wt% yielded slurry viscosity of 1628 MPA·s at shear rate of 20 s^{-1} , which was feasible for gelcasting without noticeable casting defects. The freshly gelled bodies were demolded, carefully dried, and then sintered at different schedules in nitrogen atmosphere. The reduction-sintered samples were re-sintered in air for comparative evaluation of physical property. The sintered alumina body was characterized by electrical resistance, X-ray diffraction, and scanning electron microscopy. The results showed that monomer additions and sintering schedule significantly affect in lowering electrical resistivity. The obtained lowest value was $3.6 \times 10^6 \text{ } \Omega\text{-cm}$ with 8.04 wt% monomer dosage and sintering at 1550°C with 2 h holding time. The resulting material is classified as semi-conductive, which is potential for electrostatic shielding applications. The effect of physical property and microstructure on electrical conductivity and the corresponding reaction mechanism were discussed in details. © 2006 Springer Science + Business Media, Inc.

1. Introduction

Semi-conductive materials are those materials whose electrical resistances fall in the range from $10^8 \text{ } \Omega\text{-cm}$ to $10^{-3} \text{ } \Omega\text{-cm}$ (ohm-centimeter). Various materials have conductivity in the specified range but conductive ceramics is attracting industrial interest because of its excellent performances in low and high temperature systems. Among the class of ceramic materials, alumina is commonly used because of its excellent physical properties. Although alumina has desirable physical properties, it poses difficulty in machining and surface modification due to high hardness. If alumina ceramics has electrical conductivity, it has a potential application for electrical discharge machining (EDM) [1], reaction zone separators or solid electrolytes, and even electronic materials of high electrical conductivity. Thus, there is a need to make electrically conductive alumina by without affecting its superior physical property to meet service application requirements.

Presently the fabrication of electrically conductive ceramics is done by adding metals or conductive metallic oxides to create a conductive pathways or network in ceramic matrix. Mikeska K. reported such a typical method [2] that incorporated chromia and magnesia in trace amounts to alumina and the obtained alumina is suitable for use as target electrodes in electrostatic fiber charging. The resulting conductive ceramic exhibited volume resistivity of 10^6 to $10^7 \text{ } \Omega\text{-cm}$ or less at 20°C , and has excellent electrical stability and superior mechanical properties. In a unique method, instead of adding conductive component into insulating ceramic matrix, the conductive component is used as host matrix to allow the insulating ceramic phase to form. This is done by manipulating the sintering atmosphere yielding a conductive reaction-sintered ceramics. This is typically described in a U.S. patent by Yoshiyuki *et al.* [3] in fabricating conductive nitride ceramics. In this work a molding consist of organic binder and at least one metal component powder

*Author to whom all correspondence should be addressed.

mix, which is heated under nitriding gas atmosphere consisting of nitrogen and/or ammonia, and if necessary with hydrogen, argon, helium with no CO gas. These metals are any of Ti, Zr, V, Nb, Ta, Cr, Ce, Al, Si, Hf, W, Mo, Fe, Pr, Nd, Sm, Eu, Gd, Tb, Dy, Ho, Yb, Lu, Th, and Ni. The method showed promising results of low electrical resistivity (3×10^{-5} to $1 \times 10^{-4} \Omega\text{-cm}$) and strength ranges from 340 MPa to 360 MPa, which is strong enough for electrically conductive ceramic applications. Despite of easy fabrication and high conductivity presented in the aforementioned studies, they confronted with several limitations such as segregation of components and unwanted phase formation, which results into mechanical fragility and brittleness in ceramics material. Moreover, the fabrication methods employed can cause anisotropy in electrical conductivity, low reproducibility, and it is difficult to attain ideal conductive structure by mechanical mixing. Considering the above limitations there is a strong need for a new process and hence, in this investigation, it has been attempted to make conductive ceramics by taking advantages of the known fabrication process.

Gelcasting is known widely as a forming method for dense and porous ceramics by use of *in situ* polymerization reaction, which creates three-dimensional network structure of polymer gel in the slurry [4, 5]. The gel matrix keeps on immobilizing the slurry into the desired shape of the mold, until it is strong enough for removal. The gelcasted part is then dried and heated slowly to decompose the polymer completely, and to avoid cracking defect. Subsequently, the monomer free gelcasted part is sintered in an air at high temperature to achieve high density and excellent strength.

In the present study, we propose a new process to fabricate electrically semi-conductive alumina ceramics by gelcasting and reduction sintering. This new process could possibly change a polymer network in gel-casted sample to carbon network. This carbon network is expected to provide well-continuous conductive pathways through the alumina matrix. Green alumina bodies were gel-casted in a controlled *in situ* solidification process. The resulting samples were carefully dried and sintered in a nitrogen atmosphere.

2. Experimental

2.1. Material and chemicals

The starting raw material was alumina (AL 160SG-4, M/s Showa-Denko Co., Tokyo, Japan) with mean particle

TABLE II Total carbon originating from gelcasting chemicals

Components of Slurry	Basis: 100 grams of slurry			Carbon content (g/100 grams of slurry)		
	S1	S2	S3	C1	C2	C3
Alumina	82.98	80.69	78.53	–	–	–
Distilled Water	13.52	13.15	12.79	–	–	–
Dispersant (APC)	0.51	0.49	0.48	0.08	0.08	0.08
Monomer (MAM)	2.83	5.50	8.04	1.60	3.11	4.54
Cross-Linker (MBAM)	0.14	0.14	0.13	0.08	0.08	0.07
Initiator (APS)	0.01	0.01	0.01	0.01	0.01	0.01
Catalyst (TEMED)	0.01	0.01	0.01	–	–	–
Total carbon supplied				1.77	3.27	4.70

S, represents slurry mixtures with increasing methacrylamide monomer dosages.

C, represents total initial carbon content corresponding to each slurry compositions.

size (D_{50}) of $0.60 \mu\text{m}$. The polymer dispersant used in this study was ammonium salt of polycarboxylate (M/s, Chukyo-Yushi, Nagoya, Japan) in aqueous medium. The essential gelcasting chemicals were reactive organic monomer, and cross-linker such as methacrylamide, and difunctional N,N'-Methylenebisacrylamide, respectively. The organic monomers were then initiated and catalyzed in the slurry using ammonium persulfate and N,N,N',N'-Tetramethylethylenediamine, respectively. The details of the gelcasting chemicals [5] and its respective chemical formulas are listed in Table I. Given the proportions of each chemical component in the final slurry recipe being implemented, one can approximate the amount of carbon supplied that is originating from gelcasting chemicals (Table II), which is useful in deciding the amount of monomer to be added.

2.2. Slurry preparation and gelcasting process

The alumina slurry preparation, equipment, and subsequent gelcasting process were similar to those described in the previous studies [4–6]. In this study, the conventional gelcasting process was slightly modified by varying the amount of methacrylamide monomer at three levels in increasing dosages in the premix solution. The premix solution started with 18.01 wt% premix of monomer and cross-linker in 4.55:1.00 ratio in water based on the previous study [5]. This served as a reference for varying the monomer in increasing manner (30.01 and 38.98 wt% in the premix solution) while the other components in the corresponding slurry were kept constant. To allow

TABLE I Gelcasting chemicals used for slurry preparations

Chemicals	Symbol	Chemical formula
Ammonium Polycarboxylate	APC	$\text{H}_3\text{C}(\text{HC}_2\text{O}_2\text{H}_2\text{CNH}_4)_n\text{CH}_3$
Methacrylamide	MAM	$\text{CH}_2=\text{C}(\text{CH}_3)\text{CONH}_2$
N,N'-Methylenebisacrylamide	MBAM	$(\text{CH}_2=\text{CHCONH})_2\text{CH}_2$
N,N,N',N'-Tetramethylethylenediamine	TEMED	$(\text{CH}_3)_2\text{NCH}_2\text{CH}_2\text{N}(\text{CH}_3)_2$
Ammonium Persulfate	APS	$(\text{NH}_4)_2\text{S}_2\text{O}_8$

freedom in preparing the slurry at any weights the slurry recipe was expressed per 100 g of slurry as listed in Table II. The three levels correspond to the three slurries with designation S1, S2, and S3, which also represents their corresponding gelled, dried, and sintered samples. The slurry recipes were formulated to supply at least 1.77 wt% total initial carbons relative to the mass of the slurry with designation C1, C2 and C3 in Table II.

The preparation of the slurry began with preparing the premix solution by dissolving the monomers, and cross-linker in polyethylene bottle. Initially the bottle was loaded with dispersant, distilled water and zirconia balls (1:1 ratio to powder) with amount in accordance with the intended solid loading. Manual mixing was conducted in order to dissolve the monomers. At this stage, part of the alumina powder (about 80 wt% of its weight) was then loaded into polyethylene bottle containing the premix solution and balls for milling. After two hours, the remaining powder was added in steps as the milling progressed until the whole of the intended amount had been added. All slurries were milled for at least 12 h. Correspondingly, the rheological behavior of each slurry were studied after 12 h of milling by measuring their viscosity and shear stress as a function of varying shear rate (until 110/s) of the slurry using rotational viscometer (Model: RheoStress 600, M/s Haake, Karlsruhe, Germany). The milled slurry was screened by passing through 200-mesh screen to remove the balls. This was followed by 10 min devacuation to remove the trapped air bubbles. In this stage, the slurry temperature was kept between 0°C to 1°C to avoid evaporation of water. The resulting slurry was manually added with initiator in 10% solution and catalyst, manual mixing for 5 min, and then the final slurry was immediately casted into polyurethane plastic mold. Five cylindrical plastic moulds were chosen each with height 40 mm and diameter of 20 mm. The slurry was kept under *in situ* solidification in the plastic mold for 3 h at 25°C to achieve gelation. Then, the freshly gelled body was removed and subjected to predetermined drying condition to avoid drying cracks.

2.3. Drying and sintering schedule

The controlled humidity drying was implemented for 4 days from 90% to 60% that was decreased by 10% per day, and then the weight was made to constant at 110°C to ensure moisture removal. The well-dried cylindrical samples were sintered in programmable furnace with 0.8 liter per minute flow of nitrogen (99.99% purity) following the pre-optimized sintering schedule. This was done by increasing at a rate of 12°C/min to 1100°C, and continued at 0.5°C/min to 1300°C and 1550°C with cooling rate of 12°C/min. The holding time at 1100°C and 1300°C was 2 h while at 1550°C were 2, 4 and 6 h. The cooling rate in all cases was the same. Samples sintered in nitrogen were re-sintered in an air atmosphere at 1550°C with 2 h holding time for comparative evaluation of physical properties.

2.4. Physical properties and electrical conductivity characterization

The bulk density was measured according to the weight and the dimension of the cylindrical sintered body. The relative shrinkage was determined using the lateral shrinkage along the height of the cylindrical sintered sample. All values were reported as the average of five measurements. The sintered cylindrical samples were cut into a disk (thickness: 4.0 mm, diameter: 17.0 mm) using diamond cutter (Maruto Instrument Co. Ltd.). The disk as shown in Fig. 6b was sandpaper polished to have uniform electrical contacts. The two-probe method was used for electrical resistance measurement. A silver paste was spread on both cross-sectional ends of the disks with the aid of an applicator and then the two copper electrodes were attached on the center of the disk forming a complete circuit. Then it was followed by 5 min drying at 100°C to ensure adhesion. Through these electrodes a direct current voltage ($V = 1$ volt) was applied and current (I) was measured after 10 s using LCR meter (Hewlett Packard, 4284A capacity about $10^8 \Omega\text{-cm.}$). Through these data, the electrical resistivity, (ρ) can be computed as:

$$\rho = R \frac{A}{T} (\Omega\text{-cm. unit}) \quad (1)$$

The variables in this equation include cross-sectional area of disk (A), thickness of the disk (T) and the resistance offered by the sample (R). Sintered samples were examined by powder x-ray diffractometer (RINT, Rigaku, Japan, $\text{CuK}\alpha$, 40 keV, 30 mA) to determine the phases responsible for conductivity. Scanning electron microscopy (JEOL JSM-6100) was performed on uncoated (no gold sputtering) samples in order to have clear observation of the conductive path. Furthermore, the effects of the sintering conditions (temperature and holding time) and amount of monomer on electrical resistance were investigated.

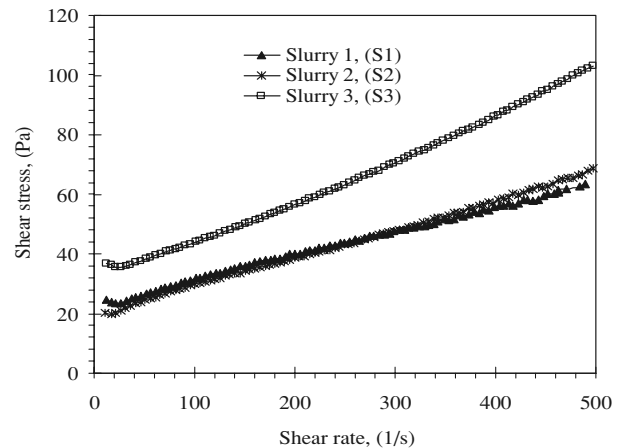


Figure 1 Shear stress versus shear rate flow curves for the three slurries.

3. Results and discussion

3.1. Rheological properties

Rheological properties of alumina slurry treated with varying dosages of monomer were evaluated after about 12 h of milling for solids loading at 78.53 to 82.98 wt%. The milling was conducted in order to break down the agglomerates and fully disperse the dispersant and gel-casting chemicals on the surface of alumina particles for achieving good slurry homogeneity. Fig. 1 depicts the flow behaviour of the three slurries containing different monomer dosages. The gelcasting slurries S1 and S2 exhibited almost of the same rheological behaviour in terms of shear stress and shear rate property. However, the viscosity of the slurry S3 is appreciably shifted higher as compared to other two slurries. This is an indication that fluidity of slurry will yield a slightly poor flow during casting. This pronounced effect may be due to the decreasing mobility of the particle when higher dosage of monomer is added. This is because of the fact that the higher the monomer dosage, the decrease in water content in the premix solution and thereby increasing the viscosity of the solution. Other possibility is that the monomer may screen the charge developed by the powders in solution, or some maybe preferentially adsorbing onto the surface of the powders, which ultimately cause low mobility of the particle [6]. Correspondingly, the viscosities of the three slurries are plotted as a function of varying shear rates, as shown in Fig. 2. It can be observed that all of the gelcasting slurries displayed shear thinning behaviour (apparent viscosity decreases with increasing shear rate) typical for ceramic suspensions containing high solids loading. Concentrated stable suspensions of this type usually exhibit the shear thinning behavior due to perturbation of the suspension structure by shearing force. At a shear rate of about 20/s, the viscosities were 1068, 959, and 1628 MPA·s corresponding to increasing monomer additions. It can be noted that good dispersion was achieved on slurry S2 with viscosity of 959 MPA·s as compared to

those of other two dosages. Further dosage at 8.04 wt% monomer (S3) yielded slightly higher slurry viscosity, but flowable with viscosity closer to 1500 MPA·s at shear rate of 20/s [7] that is the convenient range for gelcasting. This higher amount of monomer dosage (8.04 wt%) was considered because it supplied higher initial carbon (C3 in Table II) necessary for conductive pathways in alumina matrix. As a general assessment, all of the gelcasting slurries were castable without noticeable casting defects, and hence fabrication of conductive ceramics in the range of monomer chosen was feasible.

3.2. Electrical conductive property

The dried samples S1 were sintered at 1100°C and 1300°C and their electrical resistivity were listed in Table III with 2 h holding time. Additional samples were sintered at 1550°C with varying holding time 2, 4, 6 h and they had electrical resistivity listed in Table III. The rest of the samples S2 and S3 were sintered at 1550°C with 2 h holding time in order to observe the trend in electrical resistances. The electrical resistivities were found to have dramatic decrease with values of $4.80 \times 10^6 \Omega\text{-cm}$ and $3.57 \times 10^6 \Omega\text{-cm}$ as compared to pure alumina sintered in air, which is about $10^{12} \Omega\text{-cm}$. The decrease in electrical resistivity is because of the fact that increasing monomer dosage provided higher carbon network concentration regardless of sintering conditions. As reported above the obtained electrical resistance of the samples can be classified as semi-conductive material. This alumina ceramics has a potential application for electrostatic charging which use material of low electrical conductivity.

The trend of decreasing electrical resistivity with increasing sintering temperature and holding time suggested that a carbon network was gradually formed until its final conductive network in the alumina matrix at high temperature. During this process, the as-formed polymer networks encapsulate the alumina particles inherently

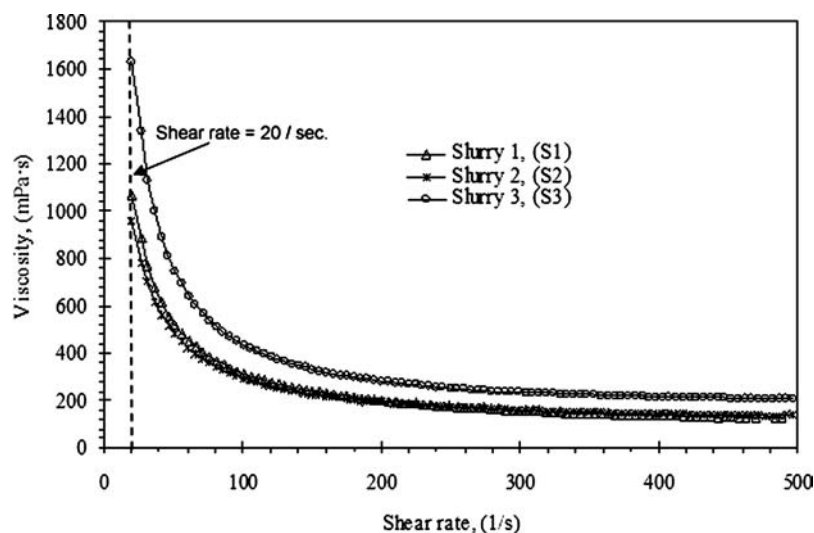


Figure 2 Viscosity versus shear rate flow curves for the three slurries.

TABLE III Electrical resistance of samples sintered in nitrogen under different sintering schedules

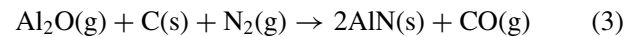
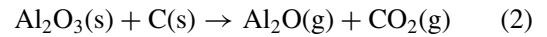
Sintering schedule	Electrical resistance ($\Omega\text{-cm}$)
1100°C on S1 with 2 h holding time	5.56×10^7
1300°C on S1 with 2 h holding time	3.69×10^7
1550°C on S1 with 2 h holding time	6.71×10^6
1550°C on S1 with 4 h holding time	6.29×10^6
1550°C on S1 with 6 h holding time	5.94×10^6
1550°C on S2 with 2 h holding time	4.83×10^6
1550°C on S3 with 2 h holding time	3.57×10^6

during gelcasting, and then by pyrolysis decomposition at high temperature transform the polymer network to carbon network through carbon precipitations. This happens by increasing temperature with accompanying grain sintering from 800°C to 1400°C in which the clusters of carbon grow and may connect by edge-to-edge linkage to form an interconnected conductive network [8]. This phenomenon is typically demonstrated in the poly-aromatic carbon network, which appears like uncompleted carbon cages enclosing the crystals of nanometer size SiC [9].

3.3. Physical, phase and microstructure effects on electrical resistance

Cylindrical samples of S1, S2, and S3 (Fig. 6a) were sintered to determine stability and revealed no sintering cracks. These provide strong evidence that our process is attractive for fabrication of semi-conductive ceramics. The sintered sample S1 was then chosen for further investigations. Fig. 3 shows the XRD patterns of sintered

S1 in nitrogen, re-sintered in air and directly sintered in an air at 1550°C with two hours soaking. The comparison of XRD pattern of sintered sample S1 in air (Fig. 3a) with sample sintered in nitrogen atmosphere (Fig. 3b) revealed six distinct peaks in addition to those peaks of pure alumina. These peaks were at 19.3°, 31.94°, 33.28°, 45.76°, and 60.64°, which correspond to aluminum nitride (AlN), while peak at 26.7° is carbon in the form of graphite. However, aluminum oxynitride phases might occur as intermediate or independent phase during sintering. The identification of this phase is quite difficult because AlN and aluminum oxynitride (AlNO) have similar lattice constants and the content was very small. The coexisting of the three phases of AlN, Al₂O₃ and C is common in the carbothermic reduction and nitridation method for the synthesis of aluminum nitride. These methods used powder mixture of alumina and carbon reacting in a flowing nitrogen stream [10], wherein this mixture described the conditions in the present study. The corresponding mechanisms are described through the following sequence of reactions as proposed by Chen and Lin [11]:



The above reactions have been known to proceed in the temperature range from 1375°C to 1552°C. According to the above mechanisms, an intermediate gas product Al₂O is formed before Al₂O₃ is converted to AlN. Most of the Al₂O eventually converted to AlN. The resulting AlN acts as coating on alumina grains along with residual

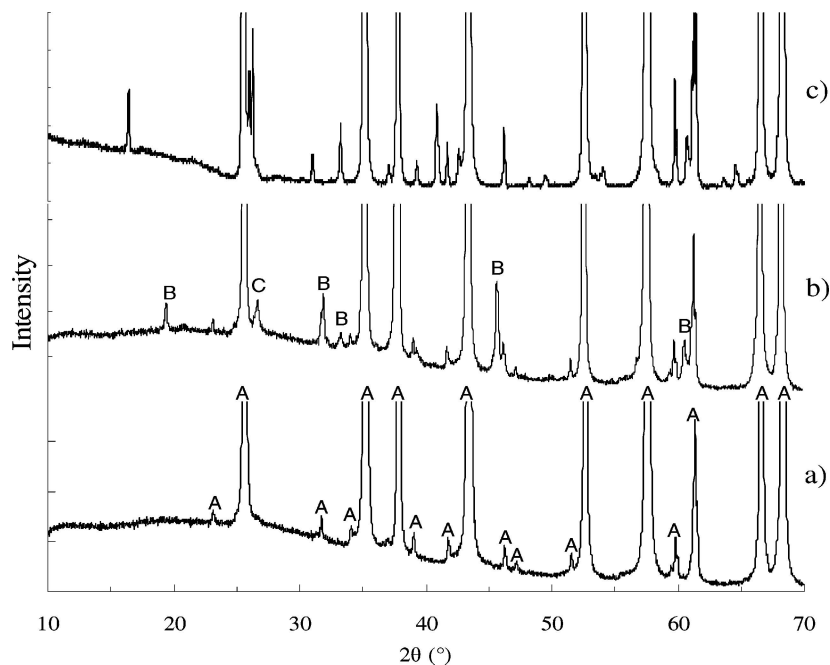


Figure 3 XRD patterns for sample S1 sintered at 1550°C with 2 h holding time. (a) sintered directly in air (b) reduction sintering (c) re-sintered in air. (A = alumina, B = AlN, C = carbon).

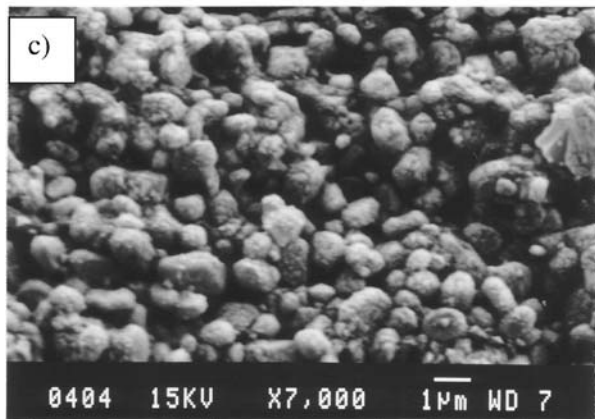
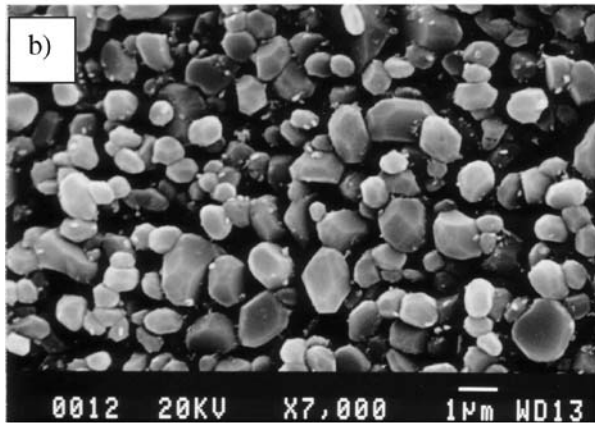
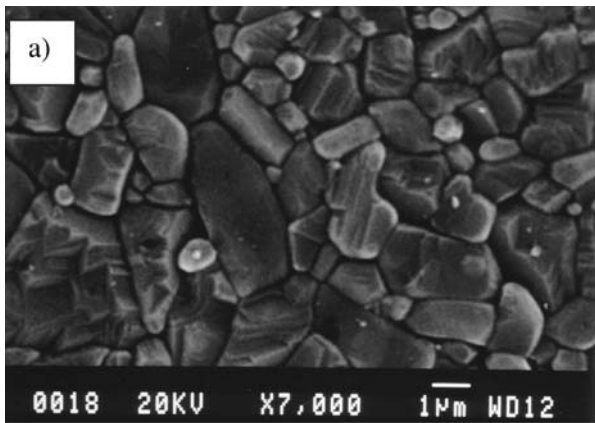


Figure 4 Microstructures of samples S1 sintered at 1550°C with 2 h holding time. (a) sintered directly in air (b) reduction sintering (c) re-sintered in air.

carbon acting as a diffusion barrier for gaseous phase. However, a small amount of Al_2O_3 diffused through the solid matrix to the surface and subsequently carried out by the nitrogen stream.

The effect of the proposed reactions were clarified by observing the microstructure of the sintered S1 in nitrogen, re-sintered in air, and directly sintered in an air at 1550°C with two hours soaking are shown in Fig. 4. It can be observed that gelcasted alumina sintered directly in air (Fig. 4a) exhibit perfect grain contacts as evidence of grain boundary connectivity, which is typical for non-conductive alumina sintered at high density. On the con-

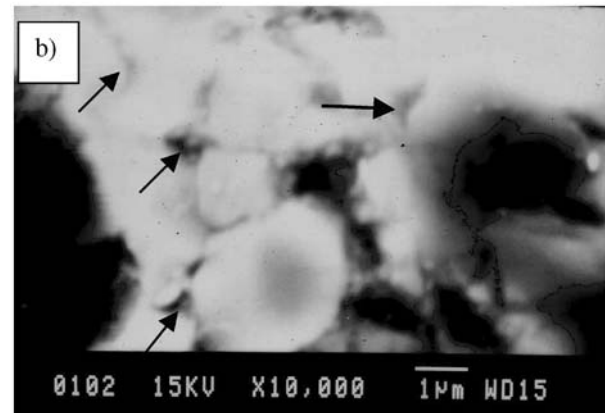
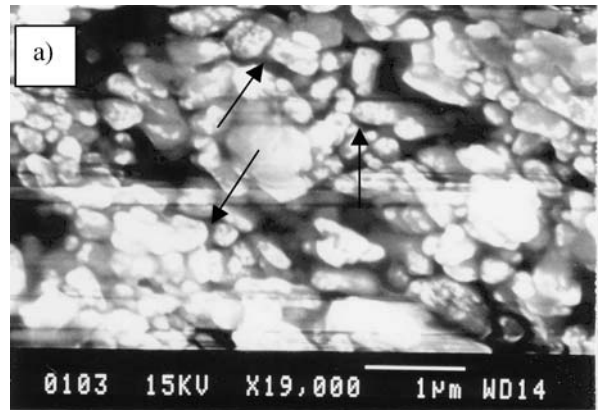


Figure 5 SEM photographs of samples S1 sintered at (a) 1100°C (b) 1550°C, showing the conductive path (pointed by arrows) with 2 h holding time.

trary, the grains of alumina sintered in reduction atmosphere are rounded morphology typical of grain growth phenomena and not in contact to each other (Fig. 4b). The grains are prevented by the interface of carbon and AlN that might result to slightly low density. Further re-sintering of the sample S1 in an air atmosphere revealed the disappearance of carbon interface and oxidation of AlN (Fig. 4c). The oxidation effects rendered the grains of alumina in globular shape with better contacts. However, the appearance did not imitate the microstructure of samples sintered directly in an air atmosphere.

The microstructures of S1 were observed at higher magnification (at least $\times 10000$) in order to view the conductive structure. Fig. 5 shows the SEM photographs of samples S1 were sintered at 1100°C and 1550°C with 2 h holding time. It can be observed in Fig. 5a the carbon coating on each alumina grains is not yet fully developed. This is corroborated with higher electrical resistivity measured at lower temperature (Table III) due to lack of network connectivity between pyrolyzed carbons. As sintering was progressed until 1550°C, the grain growth is more evident and connectivity of carbon network is more pronounced (Fig. 5b). The resulting microstructure is consistent with the appearance of different raw materials of alumina used in nitridation as reported by Li Nan and

Runzhang [13]. Moreover, it is important to note that as temperature was increased the AlN had begun to emerge as another insulating phase, which competed with carbon as coating on alumina grains. This is confirmed by XRD analysis in Fig. 3b. This typical phase assemblage is evident in SEM photograph of Fig. 5b, wherein the white areas show alumina particle coated with AlN of ash white color and black coating (pointed by arrows) on grains depicts carbon network as conductive path. This microstructure is characteristic for uncoated samples when observed microscopically the insulating phase appears white due to charging, while conductive phase becomes black. However, large black areas maybe ascribed to color contrast during analysis. Advance test on the conductive network like EDS, NMR and micro-contact impedance spectroscopy might help to validate findings and they should be recommended for further study.

The development of AlN phase explained why semi-conductive type of a material was obtained. This is because there could be a conversion of part of available carbon into gaseous phase for every conversion of AlN as expressed in the proposed sequence of reaction. The electrical resistivity of AlN is about 10^{11} Ω -cm. The onset of the proposed reactions can be slowed down by using thicker sample with increase monomer dosages. In this experiment, the sample was thick enough to provide strong diffusion barrier with more carbon to react during sintering. This can be realized by increasing the amount of carbon bearing monomer from gelcasting chemicals and the calculated carbon content increases accordingly (C1, C2, and C3) for the three slurries as presented in Table II. This is in anticipation to retain more carbon network that is conductive in alumina matrix during sintering. Indeed, the electrical resistivity decreases as much as 3.57×10^6 Ω -cm using sample S3 with two hours holding. However, the bulk densities of the sample S1, S2, and S3 that were sintered at 1550°C with 2 h holding time were decreasing, 3.67, 3.54 and 3.37 g/cm³, respectively. The decrease in bulk density was accompanied by increase linear shrinkage with increasing monomer contents and the measured values were 14.6, 15.3, and 15.9%, respectively. The increase in linear shrinkage is attributed to a higher amount of Al₂O and CO gas diffusing due to acceleration of reactions Equation 2 and 4 at the expense of Al₂O₃ phase. On the other hand, the decrease in density is due to the presence of residual carbon along with converted AlN. Both carbon and AlN are lower density phase than alumina.

Increasing the holding time on sample S1 at 1550°C, the measured electrical resistivity is decreased appreciably as shown in Table III. The lowest value of 5.94×10^6 Ω -cm was obtained using sample S1 with 6 h holding time. According to the previous studies [12, 13] that increasing the holding time produce more AlN at the expense of carbon and alumina that resulted in an increase of electrical resistance. However, the opposite trend was observed in our experiment. This is because the grains of alumina were quickly grown and compressed by the effect of increasing temperature and the presence of carbon.

Then, the reduction of porosity did not allow nitrogen gas to diffuse easily through the solid sample [12]. Therefore, the reaction rates for Equation 3 and 4 were sluggish that resulted into more residual carbon to form conductive network.

3.4. Properties of the re-sintered samples

All of the samples in the predetermined sintering schedule were re-sintered at 1550°C with 2 h holding in air for comparison of electrical resistivities. However, the electrical resistivities of all the re-sintered samples were too high and beyond the capacity of the measuring instrument (more than 10^8 Ω -cm). This is an indication that the samples became insulator similar to the alumina sintered in air with resistance about 10^{12} Ω -cm. Moreover, the sample color was changed from black to white as evidence in Fig. 6c. This is because all the AlN and carbon were oxidized leaving only alumina phase. The phases after re-sintering were confirmed by XRD pattern (Fig. 3c) and their peaks had no significant difference as compared with alumina samples sintered directly in an air atmosphere (Fig. 3a). Although in Fig. 3c it can be observed a slight difference in pattern and an extraneous peak at around 16.5°, this suggests the presence of a new phase κ -Al₂O₃ [14] polymorph in association with α -Al₂O₃. The formation of pure α -Al₂O₃ phase (Fig. 3a) was observed clearly from direct sintering of gel-casted alumina in air at 1550°C with 2 h holding. The α -Al₂O₃ phase is the last crystalline polymorph of alumina. Previous study reported [15] that alumina has several stages of transformation, and κ -Al₂O₃ is the low temperature polymorph that could readily transform to α -Al₂O₃ upon heating above 1000°C. This phase is a metastable phase of alumina at about 900°C. In this experiment, the κ -Al₂O₃ was kept unconverted to α -Al₂O₃ above 1000°C due to the combined effects of re-sintering and the presence of carbon. Moreover, κ -Al₂O₃ is the resulting phase after oxidation of AlN on the surface of α -Al₂O₃ grains that resulted into globular morphology as shown in Fig. 4c.

4. Conclusion

The combination of gel casting and reduction sintering proves to be an attractive and new process to fabricate electrically semi-conductive alumina ceramics. The process demonstrated that gelcasting with monomer dosage until 8.04 wt% relative to the weight of the slurry was feasible. Rheological studies of the slurry revealed a good dispersibility even at higher monomer dosage with viscosity of 1628 MPA·s at a shear rate of 20/s. Subsequent gelcasting exhibited a good castability without noticeable casting defects. It was also clarified that sintering schedules and monomer additions into the slurry significantly affect the measured electrical resistivity. The lowest measured electrical resistivity was 3.6×10^6 Ω -cm at 8.04 wt% methacrylamide monomer dosage (S3) when the body was sintered at 1550°C with 2 h holding time. This alumina ceramics is classified as semi-conductive, which

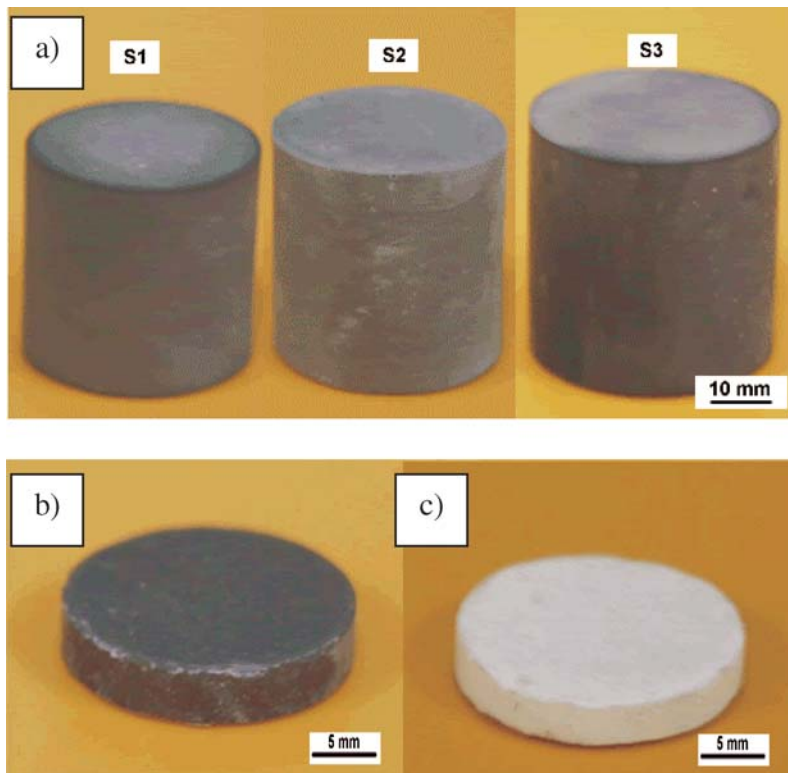


Figure 6 Photographs of samples sintered at 1550°C with 2 h holding time. (a) reduction sintered cylindrical samples (S1, S2, and S3) (b) disk sample for resistance measurement (c) re-sintered in air.

is a potential for electrostatic shielding applications. XRD analysis of the samples revealed the coexistence of three phases consisting of AlN, C, and Al₂O₃. The mechanisms of these three phases coexistence are described by the sequence of reactions as proposed by Chen and Lin [11]. The presence of AlN severely affected the electrical resistance by converting carbon to gas and thereby reduced the conductive path. SEM analysis of these three phases depicted that AlN coated Al₂O₃ grains as insulating matrix and carbon as conductive path. All the samples re-sintered in air became insulator similar to the samples sintered directly in an air. The result of XRD further shows that the phases are not different from those of samples sintered in air. This is an indication that all the AlN and carbon has been completely oxidized leaving only alumina phase.

Acknowledgements

A part of this study has been supported by a grant from the NITECH 21st Century COE Program “World Ceramics Center for Environmental Harmony” and by the Ministry of Education, Science, Sports and Culture, Grant-in-Aid for Scientific Research (B), 15310052, 2003–2005.

References

1. K. M. SHU and G. C. TU, *Int. J. Machine Tools & Manufacture* **43** (2003) 845.
2. K. R. MIKESKA, U. S. Pat. No. 5,656,203, 1997.

3. Y. K. YOSHIYUKI, M. H. TADAHIKO, S. M. MASAHISA, Y. NOBUYUKI, N. HIROSHI, T. K. KIYOHICO, A. K. SHOJI and J. FUMIO, U.S. Pat. No. 5,403,674, 1995.
3. K. R. MIKESKA, U.S. Pat. No. 5,656,203, 1997.
4. O. O. OMATETE, M. A. JANNEY and R. A. STREHLOW, *Am. Ceram. Soc. Bull.* **70** (1991) 1641.
5. M. TAKAHASHI, T. MIZUNO, Y. SHIROKI, T. YOKOYAMA, H. ABE and M. NAITO, *Ceramic Processing Science VI, Ceramic Trans.* **112** (2001) 559.
6. M. A. JANNEY, O. O. OMATETE, C. A. WALLS, S. D. NUNN, R. J. OGLE and G. WESTMORELAND, *J. Am. Ceram. Soc.* **81** (1998) 581.
7. M. POTOCZEK and E. ZAWADZAK, *Ceram. Int.* **30** (2004) 793.
8. J. CORDELAIR and P. GREIL, *J. Eur. Ceram. Soc.* **20** (2000) 1947.
9. M. MONTHIOUX and O. DELVERDIER, *ibid.* **16** (1996) 721.
10. H. K. CHEN, C. LIN and C. LEE, *J. Am. Ceram. Soc.* **77** (1994) 1753.
11. H. K. CHEN and C. I. LIN, *J. Mat. Sci.* **29** (1994) 1352.
12. *Idem.*, *ibid.* **31** (1996) 1349.
13. L. Y. LI NAN and Y. RUNZHANG, *ibid.* **34** (1999) 2547.
14. Y. YOURDSHAHYAN, C. RUBERTO, M. HALVARSSON, L. BENGSSON, V. LANGER, B. I. LUNDQVIST, S. RUPPI and U. ROLANDER, *J. Am. Ceram. Soc.* **82** (1999) 1365.
15. P. SOUZA SANTOS, H. SOUZA SANTOS and S. P. TOLEDO, *Mat. Res.* **3** (1994) 1352.

Received 24 January
and accepted 13 June 2005